

Assisted dark energy

Junko Ohashi¹ and Shinji Tsujikawa¹

¹*Department of Physics, Faculty of Science, Tokyo University of Science,
1-3, Kagurazaka, Shinjuku-ku, Tokyo 162-8601, Japan*

(Dated: November 20, 2018)

Cosmological scaling solutions, which give rise to a scalar-field density proportional to a background fluid density during radiation and matter eras, are attractive to alleviate the energy scale problem of dark energy. In the presence of multiple scalar fields the scaling solution can exit to the epoch of cosmic acceleration through the so-called assisted inflation mechanism. We study cosmological dynamics of a multi-field system in details with a general Lagrangian density $p = \sum_{i=1}^n X_i g(X_i e^{\lambda_i \phi_i})$, where $X_i = -(\nabla \phi_i)^2/2$ is the kinetic energy of the i -th field ϕ_i , λ_i is a constant, and g is an arbitrary function in terms of $Y_i = X_i e^{\lambda_i \phi_i}$. This covers most of the scalar-field models of dark energy proposed in literature that possess scaling solutions. Using the bound coming from Big-Bang-Nucleosynthesis and the condition under which the each field cannot drive inflation as a single component of the universe, we find the following features: (i) a transient or eternal cosmic acceleration can be realized after the scaling matter era, (ii) a “thawing” property of assisting scalar fields is crucial to determine the evolution of the field equation of state w_ϕ , and (iii) the field equation of state today can be consistent with the observational bound $w_\phi < -0.8$ in the presence of multiple scalar fields.

I. INTRODUCTION

The constantly accumulating observational data continue to confirm the existence of dark energy responsible for cosmic acceleration today [1]. The cosmological constant, whose equation of state is $w = -1$, has been favored by the combined data analysis of supernovae Ia [2], cosmic microwave background [3], and baryon acoustic oscillations [4]. Meanwhile, if the cosmological constant originates from a vacuum energy associated with particle physics, its energy scale is enormously larger than the observed value of dark energy ($\rho_{\text{DE}} \approx 10^{-47} \text{ GeV}^4$). Hence it is important to pursue an alternative possibility to construct dark energy models consistent with particle physics.

Scalar-field models such as quintessence [5, 6] and k-essence [7] have been proposed to alleviate the above mentioned problem. In general the energy density of a scalar field ϕ dynamically changes in time, so that its value around the beginning of the radiation-dominated epoch can be much larger than the dark energy density today. One of such models is quintessence with an exponential potential $V(\phi) = V_0 e^{-\lambda \kappa \phi}$ [8, 9], where λ is a constant and $\kappa = \sqrt{8\pi G}$ with G being gravitational constant (see Ref. [10] for the classification of cosmological dynamics and also Refs. [11] for early related papers). In fact, in higher-dimensional gravitational theories such as superstring and Kaluza-Klein theories, exponential potentials often appear from the curvature of internal spaces associated with the geometry of extra dimensions (so called “modulus” fields) [12]. Moreover it is known that exponential potentials can arise in gaugino condensation as a non-perturbative effect [13] and in the presence of supergravity corrections to global supersymmetric theories [14].

The quintessence with an exponential potential $V(\phi) = V_0 e^{-\lambda \kappa \phi}$ gives rise to two distinct fixed points in

the flat Friedmann-Lemaître-Robertson-Walker (FLRW) background [9]: (a) the scaling solution, and (b) the scalar-field dominated solution. If the slope λ of the potential satisfies the condition $\lambda > \sqrt{3(1+w_f)}$, where w_f is the equation of state of a background fluid, then the solutions approach the scaling attractor characterized by a field density parameter $\Omega_\phi = 3(1+w_f)/\lambda^2$. Even if the field energy density ρ_ϕ is initially comparable to the background fluid density ρ_f , the field eventually enters the scaling regime in which ρ_ϕ is proportional to ρ_f . This is attractive to alleviate the fine-tuning problem of the energy scale of dark energy. However the scaling solution needs to exit from the matter era to the epoch of a late-time cosmic acceleration. The scalar-field dominated solution ($\Omega_\phi = 1$) can be an accelerated attractor for $\lambda < \sqrt{2}$, but this is incompatible with the condition $\lambda > \sqrt{3(1+w_f)}$ required for the existence of scaling solutions. Hence the scaling solution cannot be followed by the scalar-field dominated solution responsible for dark energy.

There are a number of ways to allow a transition from the scaling regime to the epoch of cosmic acceleration. One of them is to introduce a single-field potential that becomes shallow at late times, e.g., $V(\phi) = c_1 e^{-\lambda \kappa \phi} + c_2 e^{-\mu \kappa \phi}$ with $\lambda > \sqrt{3(1+w_f)}$ and $\mu < \sqrt{2}$ [15] (see Ref. [16] for the classification of dynamics and Refs. [17] for related works). For this double exponential potential the field equation of state w_ϕ of the final attractor is given by $w_\phi = -1 + \mu^2/3$. In order to satisfy the observational constraint $w_\phi \lesssim -0.8$ [18] today, we require that μ is smaller than the order of 1. If the exponential potential originates from particle physics models then the slope μ is typically larger than 1, which is difficult to be compatible with the condition for cosmic acceleration.

Another way is to consider multiple scalar fields with exponential potentials, e.g., $V(\phi_1, \phi_2) = c_1 e^{-\lambda_1 \kappa \phi_1} + c_2 e^{-\lambda_2 \kappa \phi_2}$ [19, 20] (see also Refs. [21]). In fact such po-

tentials arise from the compactification of higher dimensional theories to 4-dimensional space-time. It is known that the phenomenon called *assisted inflation* [22] occurs for the multi-field exponential potential, even if the individual field has too steep a potential to lead to cosmic acceleration (see also Refs. [23]). For the sum of steep potentials satisfying the condition $\lambda_i > \sqrt{2}$ ($i = 1, 2, \dots, n$), the multiple fields evolve to give dynamics matching a single-field model with $\lambda_{\text{eff}} = (\sum_{i=1}^n 1/\lambda_i^2)^{-1/2} < \sqrt{2}$ [22]. Since the conditions $\lambda_i > \sqrt{2}$ are mostly satisfied for the models motivated by particle physics, this cooperative accelerated expansion is attractive for both inflation and dark energy. If we apply this scenario to dark energy, the scaling radiation and matter eras can be followed by the epoch of assisted acceleration as more fields join the scalar-field dominated attractor with an effective equation of state $w_\phi = -1 + \lambda_{\text{eff}}^2/3$ [20].

The scaling solution arises not only for quintessence with an exponential potential but also for more general scalar-field models with the Lagrangian density $p(\phi, X)$, where $X = -g^{\mu\nu}\partial_\mu\phi\partial_\nu\phi \equiv -(\nabla\phi)^2/2$ is a kinetic term of the field ϕ . Here $g^{\mu\nu}$ is a metric tensor with the notation $(-, +, +, +)$. It was found in Refs. [24, 25] that the existence of scaling solutions restricts the form of the Lagrangian density to be $p(\phi, X) = Xg(Xe^{\lambda\phi})$, where λ is a constant and g is an arbitrary function in terms of $Y = Xe^{\lambda\phi}$ (here we use the unit $\kappa^2 = 1$). The quintessence with an exponential potential ($p = X - ce^{-\lambda\phi}$) corresponds to the choice $g = 1 - c/Y$, whereas the choice $g = -1 + cY$ gives rise to the dilatonic ghost condensate model: $p = -X + ce^{\lambda\phi}X^2$ [25] (which corresponds to the string-theory motivated generalization of the ghost condensate model proposed in Ref. [26]). The tachyon Lagrangian density $p = -V(\phi)\sqrt{1 - 2X}$ with $V(\phi) \propto \phi^{-2}$ [27] also follows from the above scaling Lagrangian by a suitable field redefinition [28].

For the multi-field scaling Lagrangian density $p = \sum_{i=1}^n X_i g(X_i e^{\lambda_i \phi_i})$ it was shown in Ref. [29] that assisted inflation occurs with the effective slope $\lambda_{\text{eff}} = (\sum_{i=1}^n 1/\lambda_i^2)^{-1/2}$, irrespective of the form of g . Hence one can expect that the scaling solution is followed by the assisted acceleration phase for such a general Lagrangian. If we consider loop or higher-order derivative corrections to the tree-level action motivated from string theory (such as $e^{\lambda\phi}X^2$), the constant λ is typically of the order of unity [30]. In the single-field case this is not compatible with the condition for cosmic acceleration. It is of interest to see how the presence of multiple fields changes this situation.

In this paper we shall study cosmological dynamics of multiple scalar fields with the Lagrangian density $p = \sum_{i=1}^n X_i g(X_i e^{\lambda_i \phi_i})$. We are interested in the case where the scaling radiation and matter eras induced by a field ϕ_1 are followed by the dark energy dominated epoch assisted by other scalar fields. For the two-field quintessence with exponential potentials a similar analysis was partially done in Ref. [20], but we shall carry out

detailed analysis by taking into account bounds coming from Big-Bang-Nucleosynthesis (BBN) and supernovae observations. In particular the evolution of the field equation of state w_ϕ will be clarified in the presence of two and more than two fields. We also investigate cosmological dynamics for the multi-field dilatonic ghost condensate model as an example of k-essence models.

This paper is organized as follows. In Sec. II we present the dynamical equations for our general multi-field Lagrangian density without specifying any form of g . In Sec. III we derive the fixed points that correspond to the scaling radiation/matter solutions and the assisted field-dominated attractor. In Secs. IV and V we study the multi-field cosmological dynamics for quintessence with exponential potentials and the dilatonic ghost condensate model, respectively. Sec. VI is devoted to conclusions.

II. DYNAMICAL SYSTEM

Let us first briefly review single-field scaling models with the Lagrangian density $p(\phi, X)$. The existence of cosmological scaling solutions demands that the field energy density $\rho_\phi = 2Xp_{,X} - p$, where $p_{,X} \equiv \partial p/\partial X$, is proportional to the background fluid density ρ_f . Under this condition the Lagrangian density is restricted to take the following form in the flat FLRW background [24, 25]

$$p(\phi, X) = Xg(Xe^{\lambda\phi}), \quad (1)$$

where λ is a constant and g is an arbitrary function in terms of $Y \equiv Xe^{\lambda\phi}$. The Lagrangian density (1) is valid even in the presence of a constant coupling Q between the field ϕ and non-relativistic matter and also in the presence of a Gauss-Bonnet (GB) coupling between the field and the GB term¹ [31]. In the following we do not take into account such couplings. Throughout this paper we use the unit $\kappa^2 = 8\pi G = 1$.

The field density parameter for scaling solutions is given by $\Omega_\phi = 3(1 + w_f)p_{,X}/\lambda^2$ [29, 32], where w_f is the fluid equation of state. If the field enters the scaling regime during the radiation era, the BBN places the bound $\Omega_\phi < 0.045$ at the 2σ confidence level [33]. This then gives the constraint $\lambda^2/p_{,X} > 88.9$.

Besides scaling solutions, there is a scalar-field dominated point ($\Omega_\phi = 1$) with the equation of state $w_\phi = -1 + \lambda^2/(3p_{,X})$ [29, 32]. This can be used for dark energy provided that $w_\phi < -1/3$, i.e. $\lambda^2/p_{,X} < 2$. Unfortunately this condition is incompatible with the constraint coming from the BBN. Hence the scaling solution does not exit to the scalar-field dominated solution in the single-field scenario.

¹ It is also possible to obtain a generalized form of the scaling Lagrangian density even when the coupling Q between ϕ and non-relativistic matter is field-dependent [32].

If we consider multiple scalar fields ϕ_i ($i = 1, 2, \dots, n$) with the Lagrangian density

$$p = \sum_{i=1}^n X_i g(Y_i), \quad Y_i \equiv X_i e^{\lambda_i \phi_i}, \quad (2)$$

the scaling solution can be followed by the accelerated scalar-field dominated point through the assisted inflation mechanism. Even if the individual field does not satisfy the condition for inflation, the multiple fields evolve cooperatively to give dynamics matching a single-field model with [29]

$$\frac{1}{\lambda_{\text{eff}}^2} = \sum_{i=1}^n \frac{1}{\lambda_i^2}. \quad (3)$$

Since λ_{eff} is reduced compared to the individual λ_i , this allows a possibility to exit from the scaling matter era to the regime of cosmic acceleration.

In addition to the n scalar fields with the Lagrangian density (2) we take into account radiation (energy density ρ_r) and non-relativistic matter (energy density ρ_m). In the flat FLRW space-time with a scale factor a they obey the usual continuity equations $\dot{\rho}_r + 4H\rho_r = 0$ and $\dot{\rho}_m + 3H\rho_m = 0$, respectively, where a dot represents a derivative with respect to cosmic time t and $H \equiv \dot{a}/a$ is the Hubble parameter. The pressure p_{ϕ_i} and the energy density ρ_{ϕ_i} for the i -th scalar field are given, respectively, by

$$p_{\phi_i} = X_i g(Y_i), \quad (4)$$

$$\rho_{\phi_i} = 2X_i p_{,X_i} - p_{\phi_i} = X_i [g(Y_i) + 2Y_i g'(Y_i)], \quad (5)$$

where a prime represents a derivative with respect to Y_i . These satisfy the continuity equation

$$\dot{\rho}_{\phi_i} + 3H(\rho_{\phi_i} + p_{\phi_i}) = 0, \quad (6)$$

which corresponds to

$$\ddot{\phi}_i + 3HA(Y_i)p_{,X_i}\dot{\phi}_i + \lambda_i X_i \{1 - A(Y_i)[g(Y_i) + 2Y_i g'(Y_i)]\} = 0, \quad (7)$$

where

$$A(Y_i) \equiv [g(Y_i) + 5Y_i g'(Y_i) + 2Y_i^2 g''(Y_i)]^{-1}. \quad (8)$$

The Friedmann equations are

$$3H^2 = \sum_{i=1}^n \rho_{\phi_i} + \rho_r + \rho_m, \quad (9)$$

$$\dot{H} = - \sum_{i=1}^n X_i p_{,X_i} - \frac{2}{3}\rho_r - \frac{1}{2}\rho_m. \quad (10)$$

In order to derive autonomous equations we define the following quantities

$$x_i \equiv \frac{\dot{\phi}_i}{\sqrt{6}H}, \quad y_i \equiv \frac{e^{-\lambda_i \phi_i/2}}{\sqrt{3}H}, \quad u \equiv \frac{\sqrt{\rho_r}}{\sqrt{3}H}, \quad (11)$$

where the quantity Y_i defined in Eq. (2) can be expressed as

$$Y_i = x_i^2 / y_i^2. \quad (12)$$

We also introduce the field density parameters

$$\Omega_{\phi_i} \equiv \frac{\rho_{\phi_i}}{3H^2} = x_i^2 [g(Y_i) + 2Y_i g'(Y_i)], \quad \Omega_{\phi} \equiv \sum_{i=1}^n \Omega_{\phi_i}. \quad (13)$$

From Eqs. (9) and (10) it follows that

$$\Omega_m \equiv \frac{\rho_m}{3H^2} = 1 - \Omega_{\phi} - \Omega_r, \quad (14)$$

$$\frac{\dot{H}}{H^2} = -\frac{3}{2} - \frac{3}{2} \sum_{i=1}^n x_i^2 g(Y_i) - \frac{1}{2}u^2, \quad (15)$$

where $\Omega_r = u^2$ is the density parameter of radiation.

Using Eqs. (6) and (15), we obtain the autonomous equations

$$\begin{aligned} \frac{dx_i}{dN} &= \frac{x_i}{2} \left[3 + 3 \sum_{i=1}^n x_i^2 g(Y_i) + u^2 - \sqrt{6}\lambda_i x_i \right] \\ &\quad + \frac{\sqrt{6}}{2} A(Y_i) \left[\lambda_i \Omega_{\phi_i} - \sqrt{6}\{g(Y_i) + Y_i g'(Y_i)\} x_i \right], \end{aligned} \quad (16)$$

$$\frac{dy_i}{dN} = \frac{y_i}{2} \left[3 + 3 \sum_{i=1}^n x_i^2 g(Y_i) + u^2 - \sqrt{6}\lambda_i x_i \right], \quad (17)$$

$$\frac{du}{dN} = \frac{u}{2} \left[-1 + 3 \sum_{i=1}^n x_i^2 g(Y_i) + u^2 \right], \quad (18)$$

where $N = \ln(a)$. The field equation of state w_{ϕ_i} of the i -th field, the total field equation of state w_{ϕ} , and the effective equation of state w_{eff} of the system are given, respectively, by

$$w_{\phi_i} \equiv \frac{p_{\phi_i}}{\rho_{\phi_i}} = \frac{g(Y_i)}{g(Y_i) + 2Y_i g'(Y_i)}, \quad (19)$$

$$w_{\phi} \equiv \frac{\sum_{i=1}^n p_{\phi_i}}{\sum_{i=1}^n \rho_{\phi_i}} = \frac{\sum_{i=1}^n x_i^2 g(Y_i)}{\sum_{i=1}^n x_i^2 [g(Y_i) + 2Y_i g'(Y_i)]}, \quad (20)$$

$$w_{\text{eff}} \equiv -1 - \frac{2}{3} \frac{\dot{H}}{H^2} = \sum_{i=1}^n x_i^2 g(Y_i) + \frac{1}{3}u^2. \quad (21)$$

III. FIXED POINTS OF THE SYSTEM

Let us derive fixed points for the autonomous equations (16)-(18). In particular we are interested in the scaling solution and the scalar-field dominated solution. For these solutions the variables y_i do not vanish. Setting $du/dN = 0$ in Eq. (18), it follows that $u^2 = 1 - 3 \sum_{i=1}^n x_i^2 g(Y_i)$ or $u = 0$. The former corresponds to the solution in the presence of radiation, whereas the latter to the solution without radiation. In the following we shall discuss these cases separately.

A. Radiation-dominated scaling solution

Plugging $u^2 = 1 - 3 \sum_{i=1}^n x_i^2 g(Y_i)$ into Eqs. (16) and (17), the fixed point for the i -th field (with $y_i \neq 0$ and $A(Y_i) \neq 0$) satisfies

$$\lambda_i x_i = \frac{2\sqrt{6}}{3} = \frac{\sqrt{6}[g(Y_i) + Y_i g'(Y_i)]}{g(Y_i) + 2Y_i g'(Y_i)}, \quad (22)$$

which gives

$$Y_i g'(Y_i) = g(Y_i). \quad (23)$$

From Eq. (19) the field equation of state for the i -th field is

$$w_{\phi_i} = 1/3, \quad (24)$$

which means that ρ_{ϕ_i} is proportional to ρ_r . Using Eqs. (13) and (22) together with $p_{,X_i} = g(Y_i) + Y_i g'(Y_i)$, we have

$$\Omega_{\phi_i} = \frac{4p_{,X_i}}{\lambda_i^2}. \quad (25)$$

If all n scalar fields are in the scaling regime, Y_i are the same for all i ($Y_i = Y$) from Eq. (23) and hence $p_{,X_i}$ ($i = 1, 2, \dots, n$) take a common value $p_{,X} = g(Y) + Y g'(Y)$ with an effective single-field Lagrangian density $p = Xg(Y)$. Then the total field density is given by

$$\Omega_{\phi} = \frac{4p_{,X}}{\lambda_{\text{eff}}^2}, \quad (26)$$

where λ_{eff} is defined in Eq. (3). We are interested in the case where one of the fields, say ϕ_1 , is in the scaling regime in the deep radiation era, while the energy densities of other fields are suppressed relative to that of ϕ_1 . In the BBN epoch we have the following constraint from Eq. (25):

$$\frac{4p_{,X_1}}{\lambda_1^2} \lesssim 0.045 \quad \rightarrow \quad \frac{\lambda_1^2}{p_{,X_1}} > 88.9. \quad (27)$$

For a given model, i.e. for a given form of g , the variables x_1 and y_1 are determined by solving Eq. (22). If the scalar fields with $i \neq 1$ join the scaling solution at the late epoch of the radiation era, the total field density Ω_{ϕ} tends to increase according to Eq. (26) with the decrease of λ_{eff} . If the slope λ_2 of the second scalar field ϕ_2 that joins the scaling solution is of the order of 1, the field density (26) can be as large as $\Omega_{\phi} = 0.1-1$. It is not preferable for many fields with low λ_i to join the scaling solution during the radiation era in order to avoid that Ω_{ϕ} exceeds 1. This can be avoided if the field densities Ω_{ϕ_i} ($i \neq 1$) are much smaller than the radiation density.

B. Matter-dominated scaling solution and assisted scalar-field dominated point

In the absence of radiation ($u = 0$) the fixed points for the i -th field corresponding to $y_i \neq 0$ and $A(Y_i) \neq 0$ obey

the following equations

$$3 + 3 \sum_{i=1}^n x_i^2 g(Y_i) = \sqrt{6} \lambda_i x_i, \quad (28)$$

$$\lambda_i \Omega_{\phi_i} = \sqrt{6} [g(Y_i) + Y_i g'(Y_i)] x_i. \quad (29)$$

From Eqs. (13), (19), (28) and (29) it follows that

$$w_{\phi_i} = \sum_{i=1}^n x_i^2 g(Y_i) = -1 + \frac{\sqrt{6}}{3} \lambda_i x_i. \quad (30)$$

Since $w_{\phi_i} \Omega_{\phi_i} = x_i^2 g(Y_i)$ we have

$$w_{\phi_i} = \sum_{i=1}^n w_{\phi_i} \Omega_{\phi_i}. \quad (31)$$

In the case of a single field ϕ_i , this equation gives $w_{\phi_i} = 0$ or $\Omega_{\phi_i} = 1$. The former corresponds to the scaling solution along which ρ_{ϕ_i} is proportional to the matter density ρ_m , whereas the latter is the scalar-field dominated solution.

If all n scalar fields are on the fixed points characterized by the condition (30), it follows that $w_{\phi_1} = \dots = w_{\phi_i} = \dots = w_{\phi_n} \equiv w_{\phi}$ and hence $Y_1 = \dots = Y_i = \dots = Y_n \equiv Y$ from Eq. (19). In this case one has either $w_{\phi} = 0$ or $\Omega_{\phi} = 1$ from Eq. (31). Equation (30), which holds for the each scalar field, reduces to the single-field system

$$w_{\phi} = x^2 g(Y) = -1 + \frac{\sqrt{6}}{3} \lambda_{\text{eff}} x, \quad (32)$$

where $x = \lambda_i x_i / \lambda_{\text{eff}}$. The effective single-field Lagrangian density is given by $p = Xg(Y)$ with $\Omega_{\phi} = x^2 [g(Y) + 2Y g'(Y)]$. We also note that Eqs. (28) and (29) reduce to the following effective single-field forms:

$$3 + 3x^2 g(Y) = \sqrt{6} \lambda_{\text{eff}} x, \quad (33)$$

$$\lambda_{\text{eff}} \Omega_{\phi} = \sqrt{6} p_{,X} x, \quad (34)$$

where $p_{,X} = g(Y) + Y g'(Y)$.

In the following we shall discuss the matter-dominated scaling solution and the assisted field-dominated solution, separately.

1. Matter-dominated scaling solution

If the i -th scalar field is in the scaling regime during the matter-dominated epoch, i.e. $w_{\phi_i} = 0$, it follows from Eqs. (19) and (30) that $\lambda_i x_i = \sqrt{6}/2$ and

$$g(Y_i) = 0. \quad (35)$$

From Eq. (13) we obtain

$$\Omega_{\phi_i} = \frac{3p_{,X_i}}{\lambda_i^2}. \quad (36)$$

More generally the field density parameter in the presence of a perfect fluid with an equation of state w_f is given by $\Omega_{\phi_i} = 3(1 + w_f)p_{,X_i}/\lambda_i^2$ [29].

If all n scalar fields are in the scaling regime, then they can be described by an effective single-field system with $w_\phi = 0$ and

$$\Omega_\phi = \frac{3p_{,X}}{\lambda_{\text{eff}}^2}. \quad (37)$$

This scaling solution is stable for $\lambda_{\text{eff}}^2 > 3p_{,X}$ [29].

2. Assisted field-dominated point

Besides the matter scaling solution discussed above, there is another fixed point that can be responsible for the late-time acceleration. In the single-field case the solutions do not exit to the accelerated field-dominated point ($\Omega_{\phi_i} = 1$) from the scaling matter era, because the scaling solution is stable for $\Omega_{\phi_i} = 3p_{,X_i}/\lambda_i^2 < 1$. However the presence of multiple scalar fields allows this transition.

Since $\Omega_\phi = 1$ in Eq. (34) for the scalar-field dominated point with n multiple fields, it follows from Eq. (32) that

$$w_\phi = -1 + \frac{\lambda_{\text{eff}}^2}{3p_{,X}}. \quad (38)$$

This fixed point can be responsible for the late-time acceleration ($w_\phi < -1/3$) for $\lambda_{\text{eff}}^2 < 2p_{,X}$. Moreover it is stable under the condition $\lambda_{\text{eff}}^2 < 3p_{,X}$ [29] (which is opposite to the stability of the scaling matter solution). Using the relations $w_\phi\Omega_{\phi_i} = x_i^2g(Y)$ and $w_\phi = x^2g(Y)$, we find

$$\Omega_{\phi_i} = \frac{x_i^2}{x^2} = \frac{\lambda_{\text{eff}}^2}{\lambda_i^2}. \quad (39)$$

We shall study the case in which one of the fields has a large slope $\lambda_1 (\gg 1)$ to satisfy the BBN bound (27) and other fields with $\lambda_i = \mathcal{O}(1)$ join the scalar-field dominated attractor (38) at late times. Since the joining of such multiple scalar fields reduces λ_{eff} it should be possible to give rise to sufficient cosmic acceleration through the assisted inflation mechanism, even if the individual field cannot be responsible for the acceleration.

For a given model one can derive Y_1 (for the field ϕ_1) that corresponds to the scaling solution during radiation and matter eras by solving Eqs. (23) and (35), respectively. The field density parameters Ω_{ϕ_1} in these epochs are given by Eqs. (25) and (36), respectively. The assisted field-dominated solution corresponds to

$$\frac{6[g(Y) + Yg'(Y)]^2}{g(Y) + 2Yg'(Y)} = \lambda_{\text{eff}}^2, \quad (40)$$

which comes from by combining Eqs. (33) and (34) with $\Omega_\phi = 1$. By solving this equation for a given form of

$g(Y)$, we obtain the field equation of state (38) and also $x = \lambda_{\text{eff}}/(\sqrt{6}p_{,X})$ from Eq. (34).

In subsequent sections we shall consider two models: (i) quintessence with multiple exponential potentials, and (ii) the multi-field dilatonic ghost condensate model (one of k-essence models). In our numerical simulations we identify the present epoch (the redshift $z = 0$) to be $\Omega_\phi = 0.72$ with the radiation density in the region $7.0 \times 10^{-5} < \Omega_r < 1.0 \times 10^{-4}$.

IV. QUINTESSENCE WITH MULTIPLE EXPONENTIAL POTENTIALS

The single-field quintessence with an exponential potential corresponds to the Lagrangian density $p = X - ce^{-\lambda\phi}$, i.e. the choice $g(Y) = 1 - c/Y$ in Eq. (1). In the following we shall consider the Lagrangian density (2) of n scalar fields with the choice $g(Y_i) = 1 - c_i/Y_i$ ($i = 1, 2, \dots, n$).

Since $p_{,X_i} = g(Y_i) + Y_i g'(Y_i) = 1$ in this model the scaling field density Ω_{ϕ_i} during the radiation and matter eras is given by $\Omega_{\phi_i} = 4/\lambda_i^2$ and $\Omega_{\phi_i} = 3/\lambda_i^2$, respectively [see Eqs. (25) and (36)]. Below we discuss the case in which one of the scalar fields, ϕ_1 , is in the scaling regime during most of the radiation and matter eras and other fields eventually join the assisted scalar-field dominated attractor with w_ϕ given by Eq. (38). Then the BBN bound (27) gives

$$\lambda_1 > 9.42. \quad (41)$$

Under this condition, the scaling field density Ω_{ϕ_1} during the matter-dominated epoch is constrained to be $\Omega_{\phi_1} < 0.034$. If other fields join the scaling regime in the radiation (matter) era, the field density increases from $\Omega_{\phi_1} = 4/\lambda_1^2$ ($\Omega_{\phi_1} = 3/\lambda_1^2$) to $\Omega_\phi = 4/\lambda_{\text{eff}}^2$ ($\Omega_\phi = 3/\lambda_{\text{eff}}^2$). This is possible provided that the slopes of the joining scalar fields satisfy the conditions $\lambda_i \gg 1$. Meanwhile, if λ_i are of the order of 1, this leads to a large density parameter Ω_ϕ that is comparable to unity. In what follows we focus on the case in which the fields with slopes $\lambda_i = \mathcal{O}(1)$ ($i \geq 2$) enter the regime of the assisted cosmic acceleration preceded by scaling solutions induced by ϕ_1 .

It is convenient to introduce the following variable

$$\tilde{y}_i \equiv \sqrt{c_i} y_i. \quad (42)$$

From Eq. (22) the radiation-dominated scaling solution for the field ϕ_1 corresponds to

$$(x_1, \tilde{y}_1) = \left(\frac{2\sqrt{6}}{3\lambda_1}, \frac{2\sqrt{3}}{3\lambda_1} \right), \quad Y_1 = 2c_1. \quad (43)$$

This is followed by the matter-dominated scaling solution, satisfying

$$(x_1, \tilde{y}_1) = \left(\frac{\sqrt{6}}{2\lambda_1}, \frac{\sqrt{6}}{2\lambda_1} \right), \quad Y_1 = c_1. \quad (44)$$

The assisted field-dominated point corresponds to the single-field potential $V(\phi) = ce^{-\lambda_{\text{eff}}\phi}$, i.e. $g(Y) = 1 - c/Y$ with $Y = x^2/y^2$. From Eqs. (40) and (34) this is characterized by the fixed point (where we define $\tilde{y} \equiv \sqrt{cy}$):

$$(x, \tilde{y}) = \left(\frac{\lambda_{\text{eff}}}{\sqrt{6}}, \sqrt{1 - \frac{\lambda_{\text{eff}}^2}{6}} \right), \quad Y = \frac{\lambda_{\text{eff}}^2}{6 - \lambda_{\text{eff}}^2} c. \quad (45)$$

For the i -th field we have that $x_i = (\lambda_{\text{eff}}/\lambda_i)x$ and $y_i = x_i/\sqrt{Y}$.

A. Two fields

First let us consider the case of two scalar fields ϕ_1 and ϕ_2 .

In Fig. 1 we plot the evolution of the background fluid density $\rho_f = \rho_r + \rho_m$ and the field densities $\rho_{\phi_1}, \rho_{\phi_2}$ versus the redshift $z = a_0/a - 1$ (a_0 is the present value of a) for $\lambda_1 = 10$ and $\lambda_2 = 1.5$. We choose three different initial conditions for ϕ_1 . The case (i) corresponds to the exact scaling solution starting from the fixed point (43), along which $\Omega_{\phi_1} = 4/\lambda_1^2 = 0.04$ and $\Omega_{\phi_1} = 3/\lambda_1^2 = 0.03$ during radiation and matter eras, respectively. Finally the system enters the epoch in which the energy density ρ_{ϕ_2} of the second field ϕ_2 dominates the dynamics. Figure 1 shows that the field ϕ_1 eventually joins the scaling regime both for the initial conditions (ii) $\rho_{\phi_1} \approx \rho_f$ and (iii) $\rho_{\phi_1} \ll \rho_f$. Thus the cosmological trajectories converge to a common scaling solution for a wide range of initial conditions.

In Fig. 1 we find that the second field density ρ_{ϕ_2} is almost frozen after the initial transient period. In order to understand this behavior we introduce the ratio r_i between the kinetic energy $\dot{\phi}_i^2/2$ and the potential energy $V_i(\phi_i) = c_i e^{-\lambda_i \phi_i}$ of the i -th field:

$$r_i \equiv \frac{\dot{\phi}_i^2}{2V_i}, \quad (46)$$

which is related to the quantity Y_i via $r_i = Y_i/c_i$. Taking the derivative of r_i with respect to N , it follows that [34]

$$\frac{d \ln r_i}{dN} = 6[\Delta_i(t) - 1], \quad \Delta_i(t) \equiv \lambda_i \sqrt{\frac{\Omega_{\phi_i}}{3(1 + w_{\phi_i})}}. \quad (47)$$

For the scaling field ϕ_1 one has $w_{\phi_1} = w_f$ and $\Omega_{\phi_1} = 3(1 + w_f)/\lambda_1^2$ [9], where w_f is the equation of state of the background fluid. This means that $\Delta_1(t) = 1$, so that the ratio $r_1 = Y_1/c_1$ remains constant. In fact, from Eqs. (43) and (44), one has $r_1 = 2$ and $r_1 = 1$ during the radiation and matter eras, respectively. This reflects the fact that the scaling field has a kinetic energy with the same order as its potential energy.

The field ϕ_2 joining the assisted attractor at late-times satisfies $\lambda_2 = \mathcal{O}(1) \ll \lambda_1$ and $\Omega_{\phi_2} \ll \Omega_{\phi_1}$ at the early stage of the radiation era, so that $\Delta_2(t) \ll 1$ initially (unless w_{ϕ_i} is unnaturally close to -1). At this stage

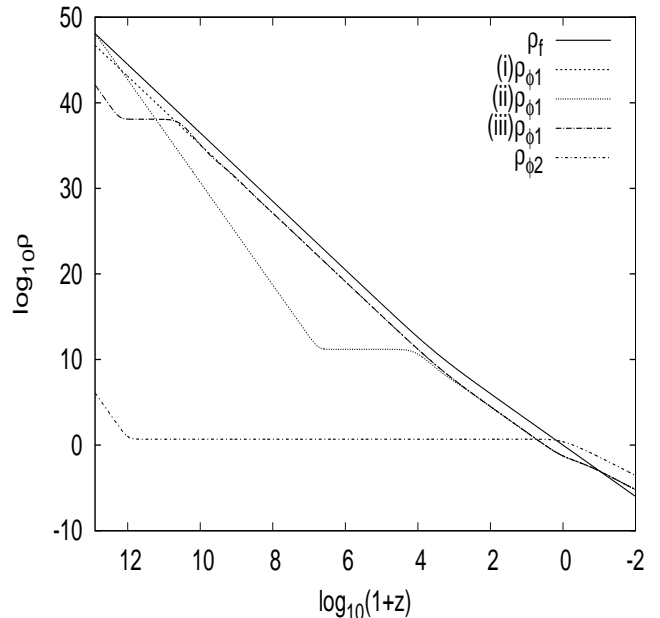


Figure 1: Evolution of the energy densities $\rho_f = \rho_r + \rho_m$, ρ_{ϕ_1} , and ρ_{ϕ_2} versus the redshift z for $\lambda_1 = 10$ and $\lambda_2 = 1.5$ in the two-field quintessence with exponential potentials. We choose three different initial conditions for ϕ_1 : (i) $x_1 = 2\sqrt{6}/(3\lambda_1)$, $\tilde{y}_1 = 2\sqrt{3}/(3\lambda_1)$, (ii) $x_1 = 0.99$, $\tilde{y}_1 = 0.12$, and (iii) $x_1 = 1 \times 10^{-3}$, $\tilde{y}_1 = 1 \times 10^{-5}$, while other initial conditions are fixed to be $x_2 = 1 \times 10^{-21}$, $\tilde{y}_2 = 2 \times 10^{-24}$, and $\Omega_m = 4 \times 10^{-10}$. In the case (i) the field ϕ_1 is in the scaling regime from the beginning.

the ratio r_2 decreases rapidly as $\propto e^{-6N}$ according to Eq. (47), see Fig. 2. In the region $r_2 \ll 1$ the field ϕ_2 is almost frozen with nearly constant ρ_{ϕ_2} . As r_2 decreases, Ω_{ϕ_2} grows and w_{ϕ_2} approaches -1 . This leads to the growth of $\Delta_2(t)$. As we see in Fig. 2 the ratio r_2 starts to increase after $\Delta_2(t)$ becomes larger than 1. When r_2 grows to the order of 1, the field ϕ_2 begins to evolve to join the assisted attractor given by Eq. (45).

The mass squared for the i -th scalar field is given by $m_i^2 \equiv d^2 V_i(\phi_i)/d\phi_i^2 = \lambda_i^2 V_i(\phi_i)$. The energy density of ϕ_2 starts to dominate around the present epoch, so that $3H_0^2 \approx V_2(\phi_2^{(0)})$ (the subscript “0” represents present values). Then the mass of ϕ_2 can be estimated as

$$m_2(\phi_2^{(0)}) \approx \lambda_2 H_0. \quad (48)$$

Recall that λ_2 needs to be of the order of 1 to realize a stable assisted attractor satisfying the condition $\lambda_{\text{eff}}^2 < 3$. Hence the mass m_2 is as small as H_0 today. In the numerical simulations of Figs. 1 and 2 the field ϕ_2 is almost frozen with the mass (48) for the redshift $1 \lesssim z \lesssim 10^{12}$ (during which the condition $r_2 \ll 1$ is fulfilled).

Even if the field ϕ_2 is rapidly rolling at the initial stage of the radiation era such that $r_2 \gg 1$, it enters the regime in which ϕ_2 is nearly frozen ($w_{\phi_2} \simeq -1$) prior to the

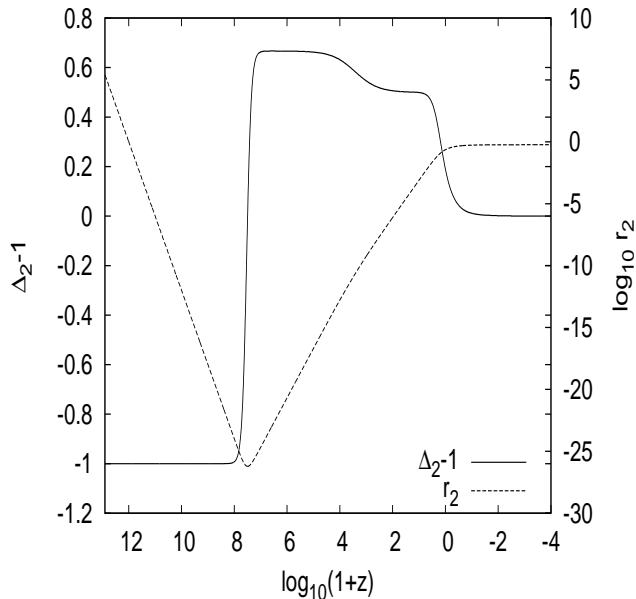


Figure 2: Evolution of r_2 and $\Delta_2 - 1$ for $\lambda_1 = 10$ and $\lambda_2 = 1.5$ in the two-field quintessence with exponential potentials. The same initial conditions are chosen as in the case (i) of Fig. 1. Initially the quantity r_2 decreases as $r_2 \propto e^{-6N}$ because $\Delta_2 \approx 0$. The ratio r_2 starts to increase after Δ_2 becomes larger than 1.

matter-dominated epoch. In Fig. 3 the evolution of ρ_{ϕ_2} is plotted for three different initial conditions of x_2 with \tilde{y}_2 fixed. The dominance of the field kinetic energy relative to its potential energy corresponds to $r_2 \gg 1$ and $w_{\phi_2} \simeq 1$, which results in the rapid decrease of Ω_{ϕ_2} to reach the regime $\Delta_2(t) \ll 1$. Even if $r_2 \gg 1$ initially, the decrease of r_2 in the regime $\Delta_2(t) \ll 1$ is so fast ($\propto e^{-6N}$) that the field ϕ_2 eventually enters the frozen regime with $w_{\phi_2} \simeq -1$. For the initial conditions satisfying $r_2 \ll 1$ the field ϕ_2 is almost frozen from the beginning, so that ρ_{ϕ_2} is nearly constant until recently.

If we change the initial conditions of \tilde{y}_2 associated with the field potential, this leads to the modification of the epoch at which the field ϕ_2 dominates at late times. This comes from the fact that the density ρ_{ϕ_2} during which ϕ_2 is nearly frozen is sensitive to the choice of its initial potential energy. Thus the evolution of the field ϕ_2 depends on its initial potential energy but not on its initial kinetic energy.

Figure 4 illustrates the variation of w_ϕ , w_{ϕ_1} , w_{ϕ_2} , and w_{eff} for $\lambda_1 = 10$ and $\lambda_2 = 1.5$ with the same initial condition as in the case (i) of Fig. 1. The equations of state w_ϕ and w_{ϕ_1} are similar to the effective equation of state w_{eff} during radiation and matter eras, but the deviation appears at low redshifts. The field ϕ_2 is almost frozen around $w_{\phi_2} = -1$ after the initial transient period, but it begins to evolve for $z \lesssim \mathcal{O}(1)$.

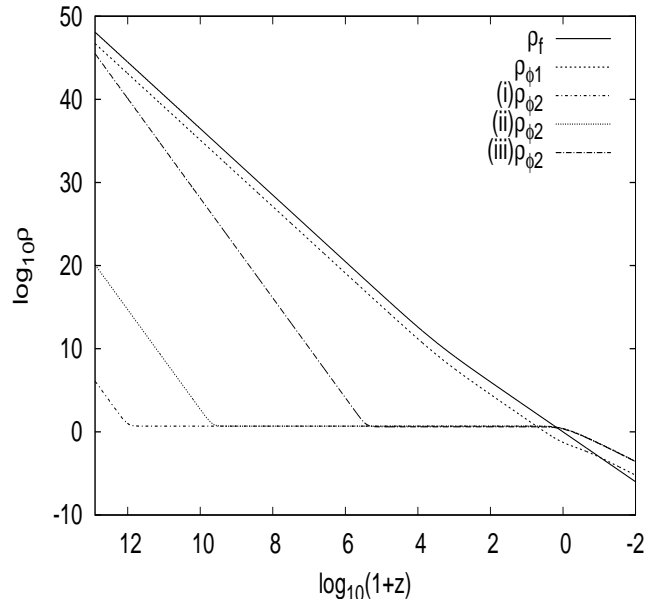


Figure 3: Evolution of ρ_f , ρ_{ϕ_1} , and ρ_{ϕ_2} for $\lambda_1 = 10$ and $\lambda_2 = 1.5$ in the two-field quintessence with exponential potentials with three different initial conditions for the kinetic energy of ϕ_2 : (i) $x_2 = 1 \times 10^{-21}$, (ii) $x_2 = 1 \times 10^{-14}$, and (iii) $x_2 = 0.05$. Other initial conditions are chosen to be $\tilde{y}_2 = 2 \times 10^{-24}$, $x_1 = 2\sqrt{6}/(3\lambda_1)$, $\tilde{y}_1 = 2\sqrt{3}/(3\lambda_1)$, and $\Omega_m = 4 \times 10^{-10}$. The field ϕ_2 enters the regime with a nearly constant ρ_{ϕ_2} independent of its initial kinetic energy.

From the definition of w_ϕ in Eq. (20) we have

$$w_\phi = \frac{1}{\Omega_\phi} (w_{\phi_1} \Omega_{\phi_1} + w_{\phi_2} \Omega_{\phi_2}). \quad (49)$$

Note that $w_{\phi_1} \approx 0$ and $w_{\phi_2} \approx -1$ around the end of the matter-dominated epoch. After Ω_{ϕ_2} gets larger than Ω_{ϕ_1} , w_ϕ begins to be mainly determined by the field ϕ_2 , i.e. $w_\phi \approx w_{\phi_2} \Omega_{\phi_2} / \Omega_\phi$. As we see in Fig. 4 w_ϕ takes a minimum before reaching the present epoch ($z = 0$), which is followed by its increase toward the attractor value $w_\phi = -1 + \lambda_{\text{eff}}^2/3$. For the model parameters used in the numerical simulation of Fig. 4 we have $\lambda_{\text{eff}} = 1.483$, which gives $w_\phi = -0.267$ at the scalar-field dominated attractor. This corresponds to the decelerated expansion of the universe. Meanwhile one has $w_\phi(z = 0) = -0.62$ and $w_{\text{eff}}(z = 0) = -0.45$, which means that the transient acceleration occurs at the present epoch. Interestingly, even without the assisted accelerated attractor, such a temporal acceleration can be realized by the presence of the thawing field ϕ_2 .

Under the BBN bound (41) and the condition $\lambda_2 > \sqrt{2}$ (i.e. the field ϕ_2 cannot be responsible for the accelerated expansion as a single component of the universe), the equation of state w_ϕ for the late-time assisted attractor is not very different from $-1/3$. Meanwhile the present value of w_ϕ is smaller than its asymptotic value. For the

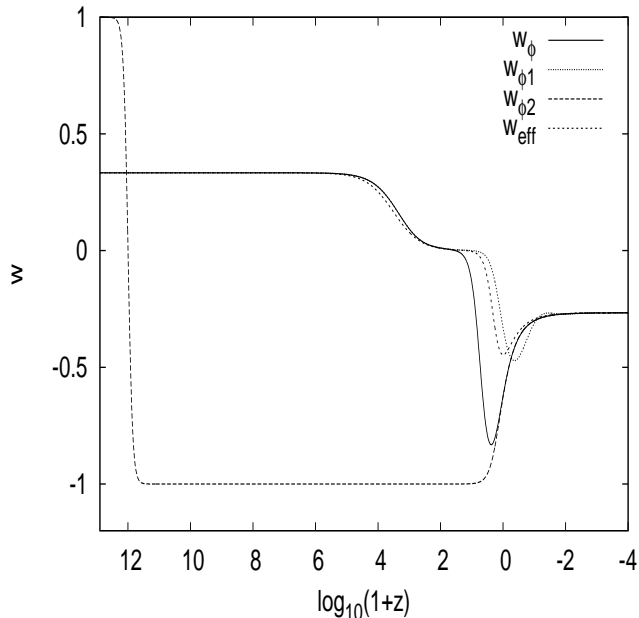


Figure 4: Evolution of the field equations of state w_ϕ , w_{ϕ_1} , w_{ϕ_2} , and the effective equation of state w_{eff} for $\lambda_1 = 10$ and $\lambda_2 = 1.5$ in the two-field quintessence with exponential potentials. The initial conditions are chosen to be $x_1 = 2\sqrt{6}/(3\lambda_1)$, $\tilde{y}_1 = 2\sqrt{3}/(3\lambda_1)$, $x_2 = 1 \times 10^{-21}$, $\tilde{y}_2 = 2 \times 10^{-24}$, and $\Omega_m = 4 \times 10^{-10}$.

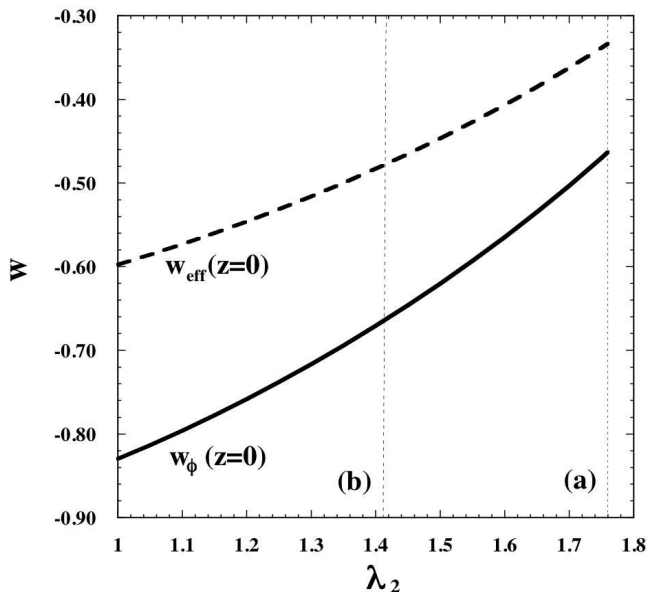


Figure 5: The field equation of state w_ϕ today versus λ_2 for $\lambda_1 = 9.43$ (solid curve) in the two-field quintessence with exponential potentials. If $\lambda_2 < 1.76$ the scalar-field dominated point is the final attractor. The condition for cosmic acceleration ($w_{\text{eff}}(z=0) < -1/3$) is satisfied even for $\lambda_2 > \sqrt{2}$. The two lines (a) and (b) in the figure correspond to $\lambda_2 = 1.76$ and $\lambda_2 = \sqrt{2}$, respectively.

marginal case with $\lambda_1 = 9.43$ and $\lambda_2 = 1.415$ we find that $w_\phi(z=0) = -0.66$ numerically. For increasing λ_2 we obtain larger values of $w_\phi(z=0)$ and $w_{\text{eff}}(z=0)$, as we see in Fig. 5. If we do not impose the condition $\lambda_2 > \sqrt{2}$, then $w_\phi(z=0)$ can be smaller than -0.66 . Note that, when $\lambda_2 > 1.76$ and $\lambda_1 = 9.43$, the scalar-field dominated point ceases to be the late-time attractor. We have also carried out numerical simulations for different values of λ_1 satisfying the condition $\lambda_1 > 9.42$ and found that $w_\phi(z=0)$ and $w_{\text{eff}}(z=0)$ are insensitive to the change of λ_1 .

B. More than two fields

For three scalar fields the total field equation of state is given by $w_\phi = (w_{\phi_1}\Omega_{\phi_1} + w_{\phi_2}\Omega_{\phi_2} + w_{\phi_3}\Omega_{\phi_3})/\Omega_\phi$. If the two fields ϕ_2 and ϕ_3 with slopes $\lambda_2, \lambda_3 = \mathcal{O}(1)$ join the assisted attractor for $z \lesssim \mathcal{O}(1)$, it is possible to obtain smaller values of $w_\phi(z=0)$ and $w_{\text{eff}}(z=0)$ relative to the two-field case.

In Fig. 6 we plot the evolution of w_ϕ , w_{ϕ_i} ($i = 1, 2, 3$) as well as w_{eff} for $\lambda_1 = 9.5$, $\lambda_2 = 1.42$, and $\lambda_3 = 2.0$. The field ϕ_1 is in the scaling regime during the radiation and matter eras, which is followed by the epoch of cosmic acceleration once the energy densities of ϕ_2 and ϕ_3 are dominant. The fields ϕ_2 and ϕ_3 have been nearly frozen (except for the initial transient period) by the time they start to evolve for $z \lesssim \mathcal{O}(1)$. In the numerical simulation of Fig. 6 the energy densities ρ_{ϕ_2} and ρ_{ϕ_3} are the same order when they begin to dominate over the background fluid density. In the numerical simulation of Fig. 6 the field equation of state today is found to be $w_\phi(z=0) = -0.76$, which is smaller than the minimum value $w_\phi(z=0) = -0.66$ in the two-field case. This comes from the fact that the third field with w_{ϕ_3} close to -1 leads to smaller values of $w_\phi(z=0)$.

For the marginal model parameters $\lambda_1 = 9.43$, $\lambda_2 = \lambda_3 = 1.415$, which satisfy the conditions $\lambda_1 > 9.42$ and $\lambda_2, \lambda_3 > \sqrt{2}$, we find that $w_\phi(z=0) = -0.83$, provided the fields ϕ_2 and ϕ_3 exit from the frozen regime almost at the same time. If either ϕ_2 or ϕ_3 begins to evolve much later than another, then $w_\phi(z=0)$ tends to be larger. This case is not much different from the two-field scenario for estimating the value of $w_\phi(z=0)$, although the scalar-field dominated attractor is different. In the three-field scenario the equation of state w_ϕ for the attractor can be as small as $w_\phi \sim -0.6$ for $\lambda_2, \lambda_3 = \mathcal{O}(1)$ so that cosmic acceleration today is not transient.

In Fig. 7 we show $w_\phi(z=0)$ versus λ_i ($i \geq 2$) for $\lambda_1 = 9.43$ in the presence of multiple scalar fields. Under the condition $\lambda_i > \sqrt{2}$ the observational bound, $w_\phi(z=0) < -0.8$, can be satisfied for three fields. In the case of four fields it is possible to satisfy the same bound for $\lambda_i < 2$ ($i = 2, 3, 4$). As we add more fields, we obtain smaller values of $w_\phi(z=0)$ and $w_{\text{eff}}(z=0)$.

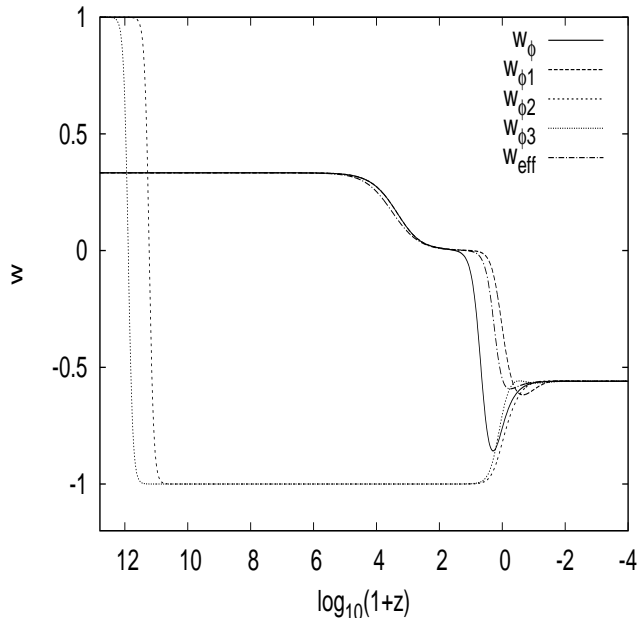


Figure 6: Evolution of w_ϕ , w_{ϕ_1} , w_{ϕ_2} , w_{ϕ_3} , and w_{eff} for $\lambda_1 = 9.5$, $\lambda_2 = 1.42$, and $\lambda_3 = 2.0$ in the three-field quintessence with exponential potentials. The initial conditions are chosen to be $x_1 = 2\sqrt{6}/(3\lambda_1)$, $\tilde{y}_1 = 2\sqrt{3}/(3\lambda_1)$, $x_2 = 1 \times 10^{-19}$, $\tilde{y}_2 = 2 \times 10^{-24}$, $x_3 = 1 \times 10^{-21}$, $\tilde{y}_3 = 2 \times 10^{-24}$, and $\Omega_m = 5 \times 10^{-10}$.

V. MULTI-FIELD DILATONIC GHOST CONDENSATE MODEL

Let us next proceed to the dilatonic ghost condensate model with n scalar fields, where the Lagrangian density is given by (2) with the choice $g(Y_i) = -1 + c_i Y_i$ ($i = 1, 2, \dots, n$), i.e. $p = \sum_{i=1}^n (-X_i + c_i e^{\lambda_i \phi_i} X_i^2)$. The coefficients c_i are positive so that the quantum instability problem of the negative kinetic energy ($-X_i$) can be avoided by the presence of the higher-order derivative term $c_i e^{\lambda_i \phi_i} X_i^2$ [24].

In this model we have $p_{,X_i} = 2\tilde{Y}_i - 1$ and

$$w_{\phi_i} = \frac{\tilde{Y}_i - 1}{3\tilde{Y}_i - 1}, \quad \Omega_{\phi_i} = x_i^2 (3\tilde{Y}_i - 1), \quad (50)$$

where

$$\tilde{Y}_i \equiv c_i Y_i. \quad (51)$$

When $\tilde{Y}_i = 1/2$ the equation of state w_{ϕ_i} is equivalent to -1 . The quantum stability of the scalar field is ensured for $\tilde{Y}_i \geq 1/2$ (i.e. $w_{\phi_i} \geq -1$), whereas in the region $\tilde{Y}_i < 1/2$ the vacuum is unstable against the catastrophic particle production of ghost and normal fields [24]. In the following we shall focus on the case $\tilde{Y}_i \geq 1/2$.

From Eqs. (16) and (17) we obtain the following equa-

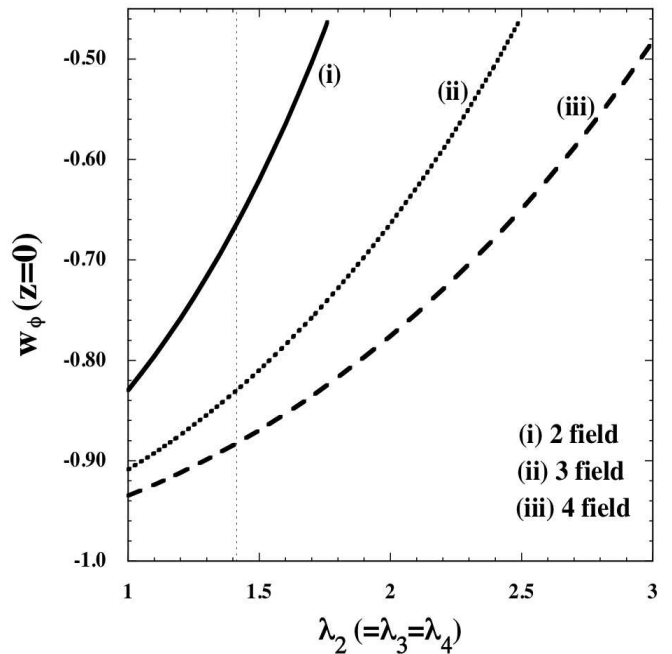


Figure 7: The equation of state w_ϕ today versus λ_i ($i \neq 1$) for $\lambda_1 = 9.43$ in the multi-field quintessence with exponential potentials. The slopes λ_i for the i -th ($i \geq 2$) fields are chosen to be the same. In this simulation the fields ϕ_i ($i \geq 2$) enter the regime of the assisted field-dominated attractor almost at the same time. Under the condition $\lambda_i > \sqrt{2}$ (which is shown as a thin dotted line in the figure), we have that $w_\phi < -0.8$ for more than two fields.

tions for \tilde{Y}_i :

$$\frac{d\tilde{Y}_i}{dN} = \tilde{Y}_i \frac{3\tilde{Y}_i(\sqrt{6}\lambda_i x_i - 4) + 6 - \sqrt{6}\lambda_i x_i}{6\tilde{Y}_i - 1}, \quad (52)$$

which hold for $i = 1, 2, \dots, n$. We will solve Eqs. (16), (18) and (52) in our numerical simulations.

For this model the solution to Eq. (23) does not exist, whereas the solution to Eq. (35) is given by $\tilde{Y}_i = 1$. This means that the scaling solution is absent during the radiation era, while it is present during the matter era. More precisely, for the background fluid with an equation of state w_f , the presence of the scaling solution corresponds to the condition $(1 - w_f)g(Y_i) = 2w_f Y_i g'(Y_i)$ [29]. Solving this equation for the present model, we obtain

$$\tilde{Y}_i = \frac{1 - w_f}{1 - 3w_f}. \quad (53)$$

For the radiation fluid ($w_f = 1/3$) we require that $\tilde{Y}_i \rightarrow \infty$ for the existence of the scaling solution. If the field ϕ_1 is in a nearly scaling regime during the radiation era, it follows that $\Omega_{\phi_1} \simeq (4/\lambda_1^2)(2\tilde{Y}_1 - 1)$. The BBN bound $\Omega_{\phi_1} < 0.045$ amounts to

$$\lambda_1 \gtrsim 9.42\sqrt{2\tilde{Y}_1 - 1}. \quad (54)$$

This shows that, under the condition $\tilde{Y}_1 \rightarrow \infty$, λ_1 needs to be infinitely large. However, as long as we do not demand the exact scaling radiation solution, the variable Y_1 can be of the order of unity (as we will see later). In such a case the constraint on λ_1 is not so restrictive.

The radiation-dominated epoch can be followed by the scaling matter era characterized by the fixed point $(x_1, \tilde{Y}_1) = (\sqrt{6}/(2\lambda_1), 1)$ with $\Omega_{\phi_1} = 3/\lambda_1^2$. The solutions finally approach the assisted field-dominated point satisfying Eq. (40), i.e.

$$\tilde{Y} \equiv cY = \frac{1}{2} + \frac{\lambda_{\text{eff}}^2}{16} \left(1 + \sqrt{1 + \frac{16}{3\lambda_{\text{eff}}^2}} \right), \quad (55)$$

where c is the coefficient of the effective single-field Lagrangian density: $p = -1 + cX$. In deriving Eq. (55) we have taken the solution with $\tilde{Y} \geq 1/2$. From Eq. (38) the field equation of state is given by

$$w_\phi = -1 + \frac{\lambda_{\text{eff}}}{2} \left(\sqrt{\lambda_{\text{eff}}^2 + \frac{16}{3}} - \lambda_{\text{eff}} \right), \quad (56)$$

which shows that the late-time cosmic acceleration occurs for $\lambda_{\text{eff}} < \sqrt{6}/3$. The stability of this solution is ensured for $\lambda_{\text{eff}}^2 < 3(2\tilde{Y} - 1)$, i.e. $\lambda_{\text{eff}} < \sqrt{3}$.

A. Two fields

We first study cosmological dynamics of the two-field ghost condensate model.

Let us consider the case in which the field ϕ_1 initially exists around $x_1 \simeq 2\sqrt{6}/(3\lambda_1)$ with a finite value of \tilde{Y}_1 satisfying the condition $\tilde{Y}_1 \geq 1/2$ [see Eq. (22)]. From Eq. (52) it follows that $d\tilde{Y}_1/dN > 0$, as long as x_1 does not depart significantly from $2\sqrt{6}/(3\lambda_1)$. This means that the quantity \tilde{Y}_1 tends to grow during most of the radiation era, which also leads to the increase of the density parameter $\Omega_{\phi_1} = x_1^2(3\tilde{Y}_1 - 1)$. This growth of \tilde{Y}_1 is associated with the fact that the radiation scaling solution exists only in the limit $\tilde{Y}_1 \rightarrow \infty$.

In Fig. 8 we plot one example about the evolution of density parameters for $\lambda_1 = 40$ and $\lambda_2 = 1$. This shows that Ω_{ϕ_1} in fact increases during the radiation-dominated epoch. In this case we have $\Omega_{\phi_1} = 0.036$ around the BBN epoch ($z \approx 10^{10}$), so that the bound $\Omega_{\phi_1} < 0.045$ is satisfied. The growth of Ω_{ϕ_1} ceases around the end of the radiation era, because \tilde{Y}_1 begins to decrease toward the scaling matter fixed point at $\tilde{Y}_1 = 1$. In order to satisfy the BBN bound (54) we have numerically found that λ_1 is required to be at least larger than 30. This is related to the fact that, even for the initial conditions of \tilde{Y}_1 close to $1/2$ around the beginning of the radiation era, \tilde{Y}_1 grows to be larger than 5 at the BBN epoch.

In Fig. 8 we find that the scaling matter era in which Ω_{ϕ_1} is nearly constant is very short, unlike the multi-field quintessence with exponential potentials. This can be

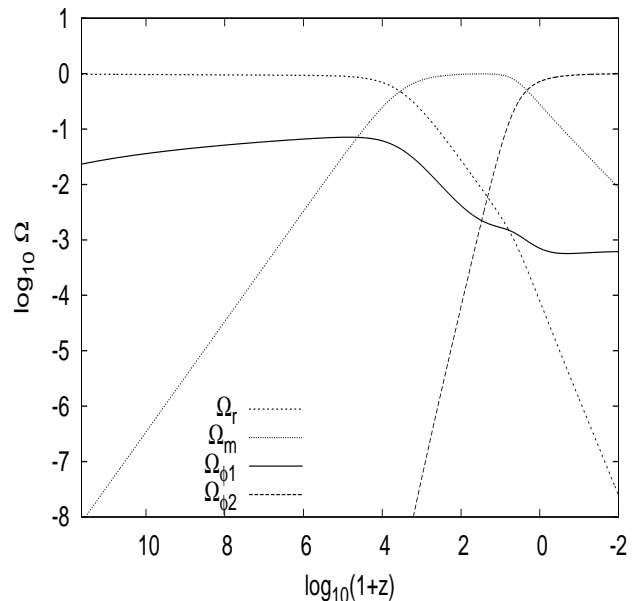


Figure 8: Evolution of Ω_r , Ω_m , Ω_{ϕ_1} , and Ω_{ϕ_2} versus the redshift z for $\lambda_1 = 40$ and $\lambda_2 = 1$ in the two-field dilatonic ghost condensate model. The initial conditions are chosen to be $x_1 = 2\sqrt{6}/(3\lambda_1)$, $\tilde{Y}_1 = 5.0$, $x_2 = 1.6 \times 10^{-20}$, $\tilde{Y}_2 = 10.0$, and $\Omega_m = 8 \times 10^{-9}$. While the BBN bound $\Omega_{\phi_1} < 0.045$ is satisfied at $z \approx 10^{10}$, the growth of Ω_{ϕ_1} continues by the redshift at $z = 7.2 \times 10^4$ with the maximum value $\Omega_{\phi_1} = 0.071$.

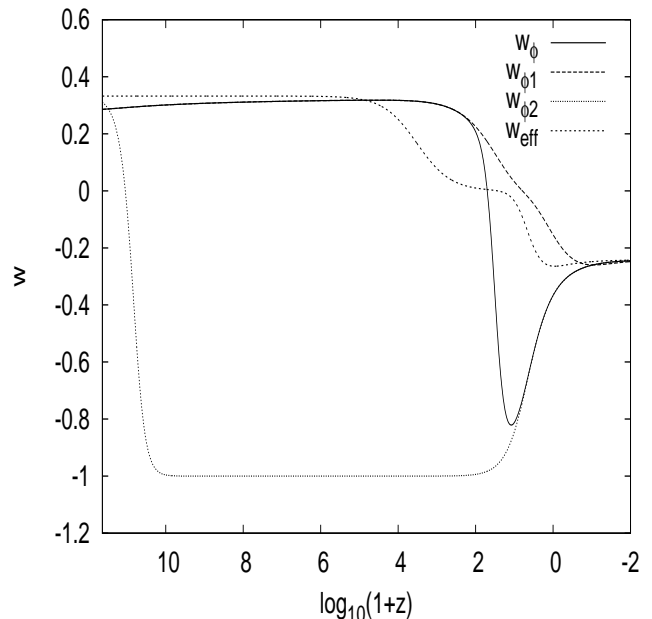


Figure 9: Evolution of w_ϕ , w_{ϕ_1} , w_{ϕ_2} , and w_{eff} for $\lambda_1 = 40$ and $\lambda_2 = 1$ in the two-field dilatonic ghost condensate model. The initial conditions are the same as in Fig. 8.

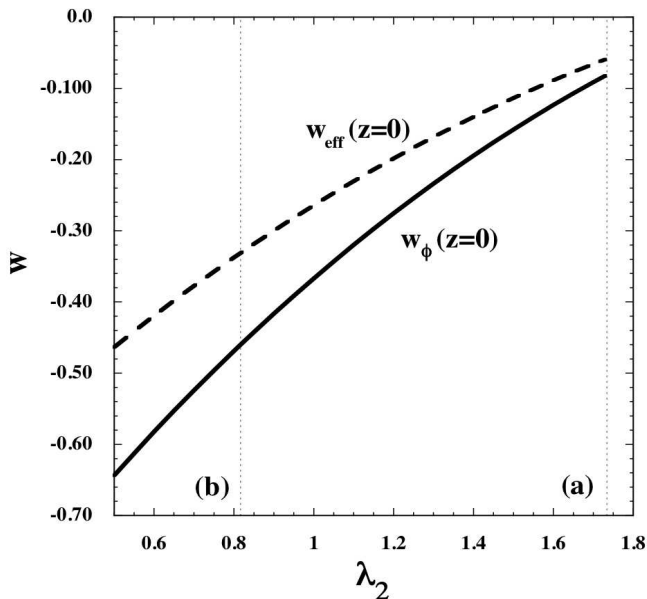


Figure 10: The equations of state w_ϕ and w_{eff} today versus λ_2 for $\lambda_1 = 40$ in the two-field dilatonic ghost condensate model. If $\lambda_2 < 1.734$ the scalar-field dominated point is the final attractor. If $\lambda_2 > \sqrt{6}/3$ the field ϕ_2 cannot be responsible for cosmic acceleration as a single component of the universe. The two lines (a) and (b) in the figure correspond to $\lambda_2 = 1.734$ and $\lambda_2 = \sqrt{6}/3$, respectively.

understood as follows. Around the end of the radiation-dominated epoch the quantity \tilde{Y}_1 has already increased to a value larger than the order of unity. It takes some time for the solutions to reach the scaling matter fixed point at $\tilde{Y}_1 = 1$. In the numerical simulation of Fig. 8 this happens for the redshift at 6.2. Since the solutions enter the dark energy dominated epoch for $z \lesssim \mathcal{O}(1)$, the period of the scaling matter era is short.

Figure 9 illustrates the evolution of w_ϕ , w_{ϕ_1} , w_{ϕ_2} , and w_{eff} for the same model parameters and initial conditions as given in Fig. 8. Initially w_{ϕ_1} is smaller than w_{eff} , but it grows to the value close to $w_{\text{eff}} = 1/3$ during the radiation era with the increase of Y_1 . The evolution of w_{ϕ_1} in Fig. 9 clearly shows that the field ϕ_1 does not soon enter the scaling matter regime just after the radiation-dominated epoch. The field ϕ_2 approaches the phase with $w_{\phi_2} \simeq -1$ after the initial transient period. This corresponds to $\tilde{Y}_2 \simeq 1/2$ and $\Omega_{\phi_2} \simeq x_2^2/2$ in Eq. (50). Numerically we find that the late-time cosmological evolution is practically independent of the initial conditions of Y_2 , but it is sensitive to the initial values of x_2 because the quantity x_2 is associated with the dark energy density.

The epoch at which the field ϕ_2 starts to exit from the regime $w_{\phi_2} = -1$ depends on the parameter λ_2 . For decreasing λ_2 the redshift z_c at which this “thawing” occurs gets smaller, which leads to smaller values of w_ϕ and w_{eff} today. In Fig. 10 we plot $w_\phi(z=0)$ and $w_{\text{eff}}(z=0)$

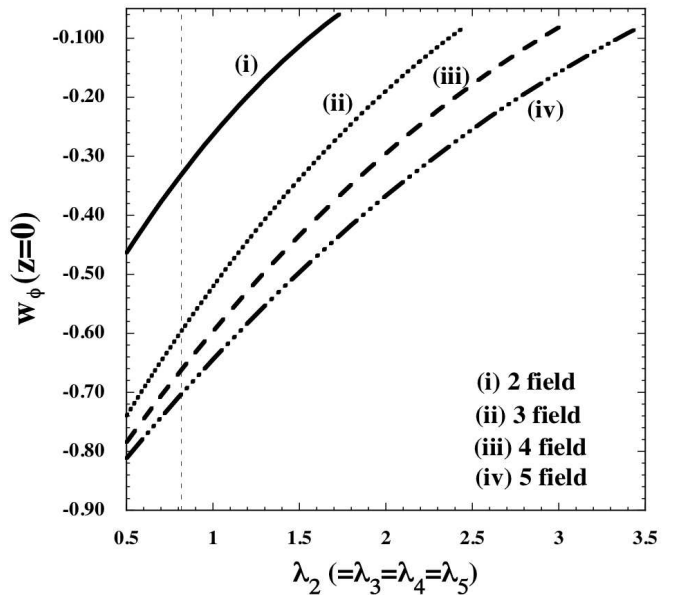


Figure 11: The equation of state w_ϕ today versus λ_i ($i \neq 1$) for $\lambda_1 = 40$ in the multi-field dilatonic ghost condensate model (up to five fields with the same slopes λ_i , $i \geq 2$). In this simulation the fields ϕ_i ($i \geq 2$) enter the regime of the assisted attractor almost at the same time. Under the condition $\lambda_i > \sqrt{6}/3$ (which is shown as a thin dotted line in the figure), it is difficult to realize $w_\phi(z=0) < -0.8$ even in the presence of five scalar fields.

versus λ_2 for $\lambda_1 = 40$. In this case the stability of the assisted field-dominated point is ensured for $\lambda_2 < 1.734$. If $\lambda_2 > \sqrt{6}/3$ the field ϕ_2 cannot drive cosmic acceleration as a single component of the universe. Under these bounds we find that the condition $w_{\text{eff}}(z=0) < -1/3$ for the acceleration today is not satisfied in the two-field case. This is intimately associated with the fact that the “thawing” of the field ϕ_2 occurs quite early ($z_c > \mathcal{O}(10)$) for $\lambda_2 > \sqrt{6}/3$, see Fig. 9. This property is different from two-field quintessence with exponential potentials in which ϕ_2 begins to evolve at smaller redshifts for the same values of λ_2 . We also note that the present values of w_ϕ and w_{eff} are insensitive to the choice of λ_1 , as long as the condition (54) is satisfied.

B. More than two fields

In the presence of more than two scalar fields it is possible to obtain smaller values of w_ϕ and w_{eff} today relative to the two-field scenario discussed above. In Fig. 11 we plot $w_\phi(z=0)$ versus λ_i ($i \geq 2$) for $\lambda_1 = 40$. The initial conditions for ϕ_i ($i \geq 2$) are chosen so that they join the assisted attractor almost at the same time. For the three-field scenario with $\lambda_2 = \lambda_3 = 0.817$ (slightly larger than $\sqrt{6}/3$) one has $w_\phi(z=0) = -0.60$ and $w_{\text{eff}}(z=0) = -0.43$, so that cosmic acceleration is realized today. However this case is difficult to be compatible

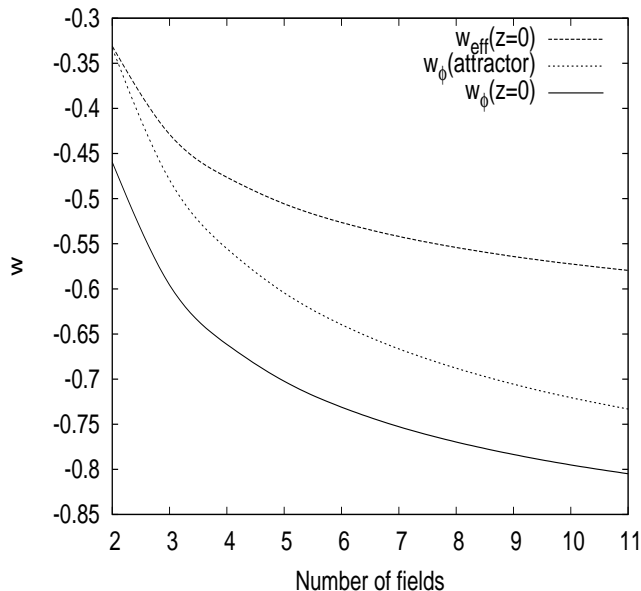


Figure 12: The present equations of state $w_{\phi}(z=0)$ and $w_{\text{eff}}(z=0)$ and w_{ϕ} at the assisted attractor versus the number n of scalar fields for $\lambda_1 = 40$ and $\lambda_i = 0.817$ ($i \geq 2$) in the multi-field dilatonic ghost condensate model. In this simulation the fields ϕ_i ($i \geq 2$) enter the regime of the assisted attractor almost at the same time.

with the observational bound $w_{\phi}(z=0) < -0.8$. Even for the five-field case with $\lambda_i = 0.817$ ($i = 2, 3, 4, 5$) we find that $w_{\phi}(z=0) = -0.70$, which is still larger than -0.8 .

In Fig. 12 we plot $w_{\phi}(z=0)$, $w_{\text{eff}}(z=0)$, and w_{ϕ} at the late-time attractor for $\lambda_1 = 40$ and $\lambda_i = 0.817$ ($i \geq 2$). This shows that we require at least 10 scalar fields to realize the condition $w_{\phi}(z=0) < -0.8$. Equation (56) leads to larger w_{ϕ} at the assisted attractor relative to the case of the multi-field quintessence with exponential potentials for the same values of λ_{eff} . In addition to the early “thawing” of assisting scalar fields, this is another reason why a large number of fields are required to realize small $w_{\phi}(z=0)$ close to -1 . In Fig. 12 we find that $w_{\phi}(z=0)$ is almost proportional to $w_{\phi}(\text{attractor})$ for $n \geq 3$. Unless we have many fields such that $n \geq 10$, $w_{\phi}(z=0)$ as well as $w_{\phi}(\text{attractor})$ are not reduced sufficiently to satisfy the observational bound. Of course, if we do not demand the condition $\lambda_i > \sqrt{6}/3$ ($i \geq 2$), it is possible to realize $w_{\phi}(z=0) < -0.8$ without introducing many fields.

VI. CONCLUSIONS

In this paper we have studied cosmological dynamics of assisted dark energy for the Lagrangian density (2) that possesses scaling solutions. This scaling Lagrangian density involves many models such as quintessence with exponential potentials, dilatonic ghost condensates, and

tachyon fields with inverse power-law potentials. As long as the energy density of a field ϕ_1 (with $\lambda_1^2 \gg p_{,X_1}$) dominates over those of other fields, the density parameter Ω_{ϕ_1} remains constant during the radiation and matter eras ($\Omega_{\phi_1} = 4p_{,X_1}/\lambda_1^2$ and $\Omega_{\phi_1} = 3p_{,X_1}/\lambda_1^2$, respectively). This property is attractive because the solutions enter the scaling regime even if the field energy density is initially comparable to the background fluid density.

In the presence of multiple scalar fields the scaling matter era can be followed by the phase of a late-time cosmic acceleration as long as more than one field join the assisted attractor. The field equation of state for the assisted attractor takes an effective single-field value $w_{\phi} = -1 + \lambda_{\text{eff}}^2/(3p_{,X})$, with λ_{eff} given by Eq. (3). Since λ_{eff} is smaller than the slope λ_i of the each field, the presence of multiple scalar fields can give rise to cosmic acceleration even if none is able to do so individually. This is a nice feature from the viewpoint of particle physics because there are in general many scalar fields (dilaton, modulus, etc) with the slopes λ_i larger than the order of unity.

While the above property of cosmological dynamics is generic for the scaling models with the Lagrangian density (2), the evolution of w_{ϕ} as well as Ω_{ϕ} is different depending on the forms of the Lagrangian density p . In order to see this we have focused on two models: (i) canonical fields with exponential potentials, and (ii) multiple dilatonic ghost condensates. These correspond to representative examples of quintessence and k-essence, respectively.

For the multi-field quintessence with exponential potentials, the slope λ_1 for the scaling field is constrained to be $\lambda_1 > 9.42$ from the BBN bound. We have numerically found that the transient cosmic acceleration today with a non-accelerated attractor can be realized after the scaling matter era. This comes from the thawing property of assisting scalar fields that start to evolve only recently from a nearly frozen regime characterized by the equation of state $w_{\phi_i} \simeq -1$ ($i \geq 2$). Even for the initial conditions where the kinetic energies of ϕ_i ($i \geq 2$) are much larger than their potential energies, we have confirmed that the fields ϕ_i enter the frozen regime by the end of the radiation-dominated epoch. In the presence of three scalar fields we have found that the total field equation of state w_{ϕ} today can be smaller than -0.8 , even if each field is unable to be responsible for the accelerated expansion as a single component of the universe.

The multi-field dilatonic ghost condensate model does not possess an exact scaling radiation era, although the scaling matter era is present. In this model the slope λ_1 of the field ϕ_1 is more severely constrained from the BBN bound relative to the multi-field quintessence with exponential potentials. The fields ϕ_i ($i \geq 2$) enter the regime characterized by $w_{\phi_i} \simeq -1$ during the radiation-dominated epoch. However the exit from this regime occurs earlier than the multi-field quintessence with exponential potentials for the same values of λ_i , which generally leads to a larger field equation of state w_{ϕ} today.

In the two-field scenario we have found that cosmic acceleration does not occur at the present epoch if the fields are unable to give rise to inflation individually. While the acceleration today is possible in the presence of more than two fields, we require at least 10 fields to satisfy the observational bound $w_\phi(z=0) < -0.8$ under the condition $\lambda_i > \sqrt{6}/3$ ($i \geq 2$).

In single-field scaling models with an exit to the late-time acceleration (such as the model in Ref. [15]), the field equation of state w_ϕ changes from 0 to negative during the transition from the matter era to the accelerated epoch. Meanwhile the multi-field dark energy models we have discussed in this paper exhibit a rather peculiar behavior of w_ϕ : it first reaches a minimum and then starts

to grow toward the assisted attractor (see Figs. 4 and 9). It will be of interest to see whether future high-precision observations will detect some signatures for such dynamics.

ACKNOWLEDGEMENTS

ST thanks Reza Tavakol for very kind hospitality during his stay in Queen Mary, University of London, where this work was partially done. We thank Hitoshi Fujiwara for useful discussions. ST thanks financial support for JSPS (No. 30318802).

-
- [1] V. Sahni and A. A. Starobinsky, *Int. J. Mod. Phys. D* **9**, 373 (2000); S. M. Carroll, *Living Rev. Rel.* **4**, 1 (2001); T. Padmanabhan, *Phys. Rept.* **380**, 235 (2003); P. J. E. Peebles and B. Ratra, *Rev. Mod. Phys.* **75**, 559 (2003); E. J. Copeland, M. Sami and S. Tsujikawa, *Int. J. Mod. Phys. D* **15**, 1753 (2006).
- [2] A. G. Riess *et al.*, *Astron. J.* **116**, 1009 (1998); *Astron. J.* **117**, 707 (1999); S. Perlmutter *et al.*, *Astrophys. J.* **517**, 565 (1999); A. G. Riess *et al.*, *Astrophys. J.* **607**, 665 (2004); P. Astier *et al.*, *Astron. Astrophys.* **447**, 31 (2006); W. M. Wood-Vasey *et al.*, *Astrophys. J.* **666**, 694 (2007); M. Kowalski *et al.*, *Astrophys. J.* **686**, 749 (2008).
- [3] D. N. Spergel *et al.*, *Astrophys. J. Suppl.* **148**, 175 (2003); E. Komatsu *et al.*, *Astrophys. J. Suppl.* **180**, 330 (2009).
- [4] D. J. Eisenstein *et al.* [SDSS Collaboration], *Astrophys. J.* **633**, 560 (2005); W. J. Percival *et al.*, *Mon. Not. Roy. Astron. Soc.* **381**, 1053 (2007).
- [5] Y. Fujii, *Phys. Rev. D* **26**, 2580 (1982); L. H. Ford, *Phys. Rev. D* **35**, 2339 (1987); C. Wetterich, *Nucl. Phys. B.* **302**, 668 (1988); B. Ratra and J. Peebles, *Phys. Rev. D* **37**, 321 (1988); T. Chiba, N. Sugiyama and T. Nakamura, *Mon. Not. Roy. Astron. Soc.* **289**, L5 (1997).
- [6] R. R. Caldwell, R. Dave and P. J. Steinhardt, *Phys. Rev. Lett.* **80**, 1582 (1998); I. Zlatev, L. M. Wang and P. J. Steinhardt, *Phys. Rev. Lett.* **82**, 896 (1999).
- [7] T. Chiba, T. Okabe and M. Yamaguchi, *Phys. Rev. D* **62**, 023511 (2000); C. Armendáriz-Picón, V. Mukhanov, and P. J. Steinhardt, *Phys. Rev. Lett.* **85**, 4438 (2000); *Phys. Rev. D* **63**, 103510 (2001).
- [8] P. G. Ferreira and M. Joyce, *Phys. Rev. Lett.* **79**, 4740 (1997); *Phys. Rev. D* **58**, 023503 (1998).
- [9] E. J. Copeland, A. R. Liddle and D. Wands, *Phys. Rev. D* **57**, 4686 (1998).
- [10] J. J. Halliwell, *Phys. Lett. B* **185**, 341 (1987).
- [11] F. Lucchin and S. Matarrese, *Phys. Rev. D* **32**, 1316 (1985); J. Yokoyama and K. i. Maeda, *Phys. Lett. B* **207**, 31 (1988); A. B. Burd and J. D. Barrow, *Nucl. Phys. B* **308**, 929 (1988).
- [12] M. B. Green, J. H. Schwarz and E. Witten, *Superstring Theory*, Cambridge University Press (1987); K. A. Olive, *Phys. Rep.* **190**, 308 (1990); E. Bergshoeff, M. de Roo, M. B. Green, G. Papadopoulos and P. K. Townsend, *Nucl. Phys. B* **470**, 113 (1996); P. Kanti and K. A. Olive, *Phys. Rev. D* **60**, 043502 (1999).
- [13] B. de Carlos, J. A. Casas and C. Muñoz, *Nucl. Phys. B* **399**, 623 (1993).
- [14] E. J. Copeland, N. J. Nunes and F. Rosati, *Phys. Rev. D* **62**, 123503 (2000).
- [15] T. Barreiro, E. J. Copeland and N. J. Nunes, *Phys. Rev. D* **61**, 127301 (2000).
- [16] L. Jarv, T. Mohaupt and F. Saueressig, *JCAP* **0408**, 016 (2004).
- [17] V. Sahni and L. M. Wang, *Phys. Rev. D* **62**, 103517 (2000); A. J. Albrecht and C. Skordis, *Phys. Rev. Lett.* **84**, 2076 (2000); S. Dodelson, M. Kaplinghat and E. Stewart, *Phys. Rev. Lett.* **85**, 5276 (2000); L. A. Urena-Lopez and T. Matos, *Phys. Rev. D* **62**, 081302 (2000); J. Barrow, R. Bean and J. Magueijo, *Mon. Not. Roy. Astron. Soc.* **316**, L41 (2000); A. A. Sen and S. Sethi, *Phys. Lett. B* **532**, 159 (2002); D. Blais and D. Polarski, *Phys. Rev. D* **70**, 084008 (2004).
- [18] S. Nesseris and L. Perivolaropoulos, *Phys. Rev. D* **72**, 123519 (2005); V. Sahni and A. Starobinsky, *Int. J. Mod. Phys. D* **15**, 2105 (2006); J. Q. Xia, G. B. Zhao, B. Feng, H. Li and X. Zhang, *Phys. Rev. D* **73**, 063521 (2006).
- [19] A. A. Coley and R. J. van den Hoogen, *Phys. Rev. D* **62**, 023517 (2000).
- [20] S. A. Kim, A. R. Liddle and S. Tsujikawa, *Phys. Rev. D* **72**, 043506 (2005).
- [21] B. Feng, X. L. Wang and X. M. Zhang, *Phys. Lett. B* **607**, 35 (2005); Z. K. Guo, Y. S. Piao, X. M. Zhang and Y. Z. Zhang, *Phys. Lett. B* **608**, 177 (2005); W. Hu, *Phys. Rev. D* **71**, 047301 (2005); R. R. Caldwell and M. Doran, *Phys. Rev. D* **72**, 043527 (2005); S. Nojiri, S. D. Odintsov and S. Tsujikawa, *Phys. Rev. D* **71**, 063004 (2005); G. Calcagni and A. R. Liddle, *Phys. Rev. D* **77**, 023522 (2008); Y. F. Cai, E. N. Saridakis, M. R. Setare and J. Q. Xia, arXiv:0909.2776 [hep-th].
- [22] A. R. Liddle, A. Mazumdar and F. E. Schunck, *Phys. Rev. D* **58**, 061301 (1998).
- [23] K. A. Malik and D. Wands, *Phys. Rev. D* **59**, 123501 (1999); E. J. Copeland, A. Mazumdar and N. J. Nunes, *Phys. Rev. D* **60**, 083506 (1999); P. Kanti and K. A. Olive, *Phys. Lett. B* **464**, 192 (1999); A. M. Green and J. E. Lidsey, *Phys. Rev. D* **61**, 067301 (2000); A. Mazumdar, S. Panda and A. Perez-Lorenzana, *Nucl. Phys. B* **614**, 101 (2001); M. C. Bento, O. Bertolami and N. M. C. Santos, *Phys. Rev. D* **65**, 067301 (2002);

- A. Collinucci, M. Nielsen and T. Van Riet, *Class. Quant. Grav.* **22**, 1269 (2005); J. Hartong, A. Ploegh, T. Van Riet and D. B. Westra, *Class. Quant. Grav.* **23**, 4593 (2006).
- [24] F. Piazza and S. Tsujikawa, *JCAP* **0407**, 004 (2004).
- [25] S. Tsujikawa and M. Sami, *Phys. Lett. B* **603**, 113 (2004).
- [26] N. Arkani-Hamed, H. C. Cheng, M. A. Luty and S. Mukohyama, *JHEP* **0405**, 074 (2004).
- [27] T. Padmanabhan, *Phys. Rev. D* **66**, 021301 (2002); J. M. Aguirregabiria and R. Lazkoz, *Phys. Rev. D* **69**, 123502 (2004).
- [28] E. J. Copeland, M. R. Garousi, M. Sami and S. Tsujikawa, *Phys. Rev. D* **71**, 043003 (2005).
- [29] S. Tsujikawa, *Phys. Rev. D* **73**, 103504 (2006).
- [30] J. E. Lidsey, D. Wands and E. J. Copeland, *Phys. Rept.* **337**, 343 (2000); M. Gasperini and G. Veneziano, *Phys. Rept.* **373**, 1 (2003).
- [31] S. Tsujikawa and M. Sami, *JCAP* **0701**, 006 (2007).
- [32] L. Amendola, M. Quartin, S. Tsujikawa and I. Waga, *Phys. Rev. D* **74**, 023525 (2006).
- [33] R. Bean, S. H. Hansen and A. Melchiorri, *Phys. Rev. D* **64**, 103508 (2001).
- [34] P. J. Steinhardt, L. M. Wang and I. Zlatev, *Phys. Rev. D* **59**, 123504 (1999).